Published in final edited form as:
Nat Med. 2002 August ; 8(8): 841–849. doi:10.1038/nm740.

Placental growth factor reconstitutes hematopoiesis by recruiting VEGFR1^{+} stem cells from bone-marrow microenvironment

Koichi Hattori[1], **Beate Heissig**[1], **Yan Wu**[3], **Sergio Dias**[1], **Rafael Tejada**[1], **Barbara Ferris**[1], **Daniel J. Hicklin**[3], **Zhenping Zhu**[3], **Peter Bohlen**[3], **Larry Witte**[3], **Jan Hendrikx**[4], **Neil R. Hackett**[1], **Ronald G. Crystal**[1], **Malcolm A.S. Moore**[2], **Zena Werb**[5], **David Lyden**[1,2], and **Shahin Rafii**[1]

[1] Department of Medicine, Cornell University Medical College, New York, New York, USA

[2] Sloan–Kettering Institute, New York, New York, USA

[3] ImClone Systems Inc., New York, New York, USA

[4] New York Blood Center, New York, New York, USA

[5] Department of Anatomy, University of California, San Francisco, California, USA

Abstract

The mechanism by which angiogenic factors recruit bone marrow (BM)-derived quiescent endothelial and hematopoietic stem cells (HSCs) is not known. Here, we report that functional vascular endothelial growth factor receptor-1 (VEGFR1) is expressed on human CD34^{+} and mouse Lin^{-}Sca-1^{+}c-Kit^{+} BM-repopulating stem cells, conveying signals for recruitment of HSCs and reconstitution of hematopoiesis. Inhibition of VEGFR1, but not VEGFR2, blocked HSC cell cycling, differentiation and hematopoietic recovery after BM suppression, resulting in the demise of the treated mice. Placental growth factor (PlGF), which signals through VEGFR1, restored early and late phases of hematopoiesis following BM suppression. PlGF enhanced early phases of BM recovery directly through rapid chemotaxis of VEGFR1^{+} BM-repopulating and progenitor cells. The late phase of hematopoietic recovery was driven by PlGF-induced upregulation of matrix metalloproteinase-9, mediating the release of soluble Kit ligand. Thus, PlGF promotes recruitment of VEGFR1^{+} HSCs from a quiescent to a proliferative BM microenvironment, favoring differentiation, mobilization and reconstitution of hematopoiesis.

Recruitment of endothelial and hematopoietic progenitors and stem cells (HSCs) from the bone-marrow (BM) microenvironment and subsequent mobilization to circulation contributes to tissue vascularization and organogenesis. We showed that release of angiogenic factors by tumor cells mobilizes BM-derived endothelial and hematopoietic cells, which promotes tumor growth[1] and suggests that angiogenic factors may also convey signals that regulate hematopoiesis.

During steady-state conditions, HSCs reside in a quiescent state[2]. Stress induction, including chemotherapy/irradiation, results in the release of chemocytokines that increase stem cell motility[3,4], thereby facilitating their entry into a microenvironment where they proliferate,

Correspondence should be addressed to S.R.; srafii@med.cornell.edu.
K.H. and B.H. contributed equally to this study.

Note: Supplementary information is available on the *Nature Medicine* website.

Competing interests statement
The authors declare competing financial interests: see the website (http://medicine.nature.com) for details.

differentiate and are mobilized to the circulation. Despite advances in phenotypic identification of pluripotent HSCs (refs. [5–7]), the molecular pathways involved in the angiogenic factor–mediated recruitment of HSCs for reconstitution of hematopoiesis are not known.

Within the vascular endothelial growth factor (VEGF) family, VEGF-A is a potent mediator of the angiogenic switch[8,9]. VEGF-A interacts with the tyrosine kinase receptors VEGF receptor-1 (VEGFR1, Flt-1) and VEGF receptor-2 (VEGFR2, Flk-1, KDR). Placental growth factor (PlGF), another member of this family, functions as an angiogenic amplifier by signaling through VEGFR1 (ref. [10]). Mice deficient in VEGFR2 display defects in vasculogenesis and hematopoiesis[11–13]. Although one study has shown that VEGFR2 is expressed on adult human $CD34^+$ NOD/SCID repopulating cells[14], murine BM-derived $VEGFR2^+$ cells have been shown to be unable to repopulate lethally irradiated recipients[15]. Therefore, the functional role of VEGFR2 expression on HSCs in the regulation of hematopoiesis remains unclear.

As $VEGFR1^{-/-}$ mice die from vascular disorganization in early embryogenesis, the role of VEGFR1 in the regulation of hematopoiesis has been difficult to evaluate[16,17]. Mice deficient in the VEGFR1-kinase domain have an angiogenic[18], but no apparent hematopoietic defect. Nonetheless, post-natal expression of VEGFR1 seems to be associated with the regulation of hematopoietic cell motility. VEGF-A induces migration of $VEGFR1^+$ myelomonocytic cells *in vitro*[19–21]. We showed that VEGF-A and/or angiopoietin-1 mobilize BM-repopulating cells[22]. In *Drosophila*, VEGF modulates primitive hematopoiesis through enhancing hemocyte motility[23]. Based on these data, we hypothesized that expression of VEGF receptors, in particular VEGFR1, regulate hematopoiesis by increasing HSC motility and recruitment.

We used a myelosuppression model where the role of PlGF and VEGF receptors in the regulation of hematopoietic reconstitution can be tested. Mice were treated with the cytotoxic agent 5-fluorouracil (5FU), which depletes cycling hematopoietic cells[24,25]. We demonstrate that functional VEGFR1, but not VEGFR2, is present on BM-repopulating HSCs. Inhibition of VEGFR1, but not VEGFR2, blocked HSC cell cycling, differentiation and hematopoietic recovery after BM suppression, resulting in the demise of the treated mice. PlGF restored hematopoiesis following myelosuppression by two distinct mechanisms. In the early phases of BM recovery, PlGF directly promoted recruitment of $VEGFR1^+$ HSC and progenitors, whereas in later stages, PlGF indirectly supported hematopoiesis through metalloproteinase-9 (MMP-9)-mediated release of soluble Kit ligand (sKitL). These studies suggest that PlGF, which is endowed with a low toxicity profile provides for a novel strategy to induce hematopoiesis after chemotherapy/radiation, or in hematological disorders such as myelodysplastic syndromes.

$CD34^+VEGFR1^+$ cells comprise of NOD/SCID-repopulating cells

Hematopoietic stem cells (HSCs) express the antigens CD34 and/or AC133. In unseparated cord blood (CB), 4% of mononuclear cells expressed both VEGFR1 and CD14, whereas a smaller cell fraction (<0.2%) stained for VEGFR1, but not for CD15 and CD14. VEGFR1 was expressed on 6.4 ± 0.5% and 4.3 ± 0.3% of human fetal liver and CB-derived $CD34^+$ and $AC133^+$ cells, respectively (Supplementary Fig. A online). $VEGFR1^+$ cells were also detected in the $CD38^-$ population, which comprises a phenotypically primitive population of HSCs.

To evaluate the pluripotency of $VEGFR1^+$ cells, human CB-derived $CD34^+$, $CD34^+VEGFR1^+$ and $CD34^+VEGFR1^-$ cells were transplanted into sublethally irradiated NOD/SCID mice. Transplantation of 10^4 human-derived $CD34^+VEGFR1^+$ cells into NOD/SCID mice resulted in long-term engraftment of human/mouse chimeric BM cells 4 months after transplantation (Supplementary Fig. B online). Eight times more cells were necessary to engraft NOD/SCID mice with $CD34^+VEGFR1^-$ cells. In the BM of NOD/SCID mice transplanted with $VEGFR1^+CD34^+$ cells (and $CD34^+$ cells), 70 days after transplantation,

12.6% ± 2.0 (20.7% ± 0.7) of BM cells expressed the human B-cell CD19, 0.3% ± 0.1 (0.4% ± 0.2) stained for the human T-cell CD3 and 4.9% ± 0.9 (8.0% ± 7.4) expressed the human myeloid CD33 and co-expressed human CD45, respectively. These data indicate that $CD34^+VEGFR1^+$ cells comprise cells with long-term hematopoietic repopulating capacity, capable of multi-lineage cell differentiation.

Short- and long-term BM-repopulating cells express VEGFR1

Murine lineage-negative Sca-1 positive ($Lin^-Sca\text{-}1^+$) cells and side population cells (SP cells) [26] are enriched for pluripotent HSCs with BM-repopulating capacity. FACS analysis revealed that 1.4% of murine unseparated BM mononuclear cells (BMMCs) stained for VEGFR1 (Fig. 1*a*). Following $Lin^-Sca\text{-}1^+$ isolation, 73.5 ± 3.1% ($n = 6$) of these cells expressed VEGFR1, 29.5% expressed c-Kit and 2.5% double-stained for VEGFR1 and VEGFR2. $VEGFR1^+$ cells were also detected in the SP cells of murine BMMCs (data not shown).

In BALB/c mice, 2 days after 5FU treatment, 5.1 ± 0.3% ($n = 6$) of BMMCs expressed VEGFR1 as compared with 1.4% prior to treatment (Fig. 1*b*). Within the $VEGFR1^+$ population, 31.4 ± 0.3% of the cells co-expressed Sca-1 and 35.7 ± 0.7% stained for c-Kit, both of which are stem cell-associated markers. To determine the BM-repopulating capacity of $VEGFR1^+$ cells, post 5FU-purified $VEGFR1^+$ BMMCs from male mice were transplanted into lethally irradiated syngeneic female mice. All mice transplanted with $VEGFR1^-$ and $VEGFR2^+$ cells died within 14 days, whereas 38%, 63%, and 100% of mice transplanted with 1×10^2, 1×10^3 and 1×10^5 of $VEGFR1^+$ BMMCs from male donors survived beyond 150 days, respectively (Fig. 1*c*). At 5 months, more than 80% of BM cells were Y-chromosome positive donor cells in female recipients transplanted with $VEGFR1^+$ BMMCs.

Similarly, congeneic transplantation of 1×10^3 $VEGFR1^+Sca\text{-}1^+$ or $VEGFR1^+Sca\text{-}1^-$ BMMCs obtained from 5FU-treated C57BL/6-Ly5.2 mice rescued lethally irradiated C57BL/6-Ly5.1 mice (Fig. 1*d*). Five months after transplantation, 88% of myeloid (CD11b, Gr-1) and lymphoid (B220, Thy-1) cells in the circulation were of $VEGFR1^+$ donor (Ly5.2) origin (Fig. 1*e*), indicating that murine $VEGFR1^+$ BM cells have short- and long-term BM-repopulating capacity.

Activation of VEGFR1 is essential for BM reconstitution

5FU-injected mice treated with IgG (controls) or monoclonal antibody to VEGFR2 had complete hematopoietic reconstitution within three weeks (Fig. 2*a*). However, 67% of mice treated with neutralizing antibody to VEGFR1 succumbed within 3 weeks after 5FU-induced BM-suppression (Fig. 2*b*). The surviving mice had profound delay in hematopoietic recovery (Fig. 2a). Treatment with either anti-VEGFR2 or anti-VEGFR1 for 4 weeks in non-5FU treated mice did not cause hematopoietic toxicity (Fig. 2*a*). These data suggest that signaling through VEGFR1, but not VEGFR2, plays a role in hematopoietic reconstitution after myeloablation.

If VEGFR1 inactivation following myelosuppression delays hematopoietic reconstitution, administration of PlGF, the ligand signaling through VEGFR1 but not VEGFR2, should improve hematopoietic recovery. Mice were treated with 5FU (Fig. 2*c*) or a combination of carboplatin and total body irradiation (TBI) (Fig. 2*d*). Following myelosuppression, elevated PlGF levels delivered by adenoviral-vector expressing PlGF (Ad-PlGF), resulted in faster WBC recovery in the early (day 0–6) and later (day 7–16) phases of BM suppression. Extent and duration of WBC recovery of less than 2000/μl was shorter in the Ad-PlGF-treated group compared with the Ad-null-treated group (Fig. 2*c* and *d*). Plasma elevation of PlGF improved WBC recovery similar to that seen after G-CSF treatment (Fig. 2*d*), except in the early phases after myelosuppression, at time points where G-CSF is proven to be ineffective[27,28].

Inhibition of VEGFR1 impairs hematopoietic recovery

The delayed hematopoietic recovery following myelosuppression was associated with a significantly reduced number of BMMCs in mice injected with anti-VEGFR1, as compared with mice treated with antibody to VEGFR2 or IgG (Figs. 2*e*, *f* and *g* and 3*a*). The BM of 5FU-treated mice injected with anti-VEGFR1 showed a decrease in lineage-committed cells, particularly in the megakaryocytic lineage (Fig. 2*h–m*).

FACS analysis of BM cells confirmed the tri-lineage suppression after treatment with blocking anti-VEGFR1. The frequency of BMMCs expressing erythroid (TER119), myeloid (CD11b, Gr1) and lymphoid (B220) markers was significantly decreased on day 6 after VEGFR1 antibody treatment as compared with IgG controls (Fig. 3*b*). There was also a delay in the erythroid and lymphoid recovery in mice receiving anti-VEGFR2, but this did not translate into increased mortality in these mice. The decreased BM cellularity in anti-VEGFR1-treated mice was due to fewer $Lin^{-}Sca\text{-}1^{+}$ (Fig. 3*c*) and $Sca\text{-}1^{+}$ cells (Fig. 3*d* and *e*) in S and G_2/M phase of the cell cycle as compared with anti-VEGFR2-and IgG-treated mice. Because 70% of the mice treated with anti-VEGFR1 succumbed to fatal complications afforded by BM failure, timely activation of the PlGF/VEGFR1 pathway is important for HSC and progenitor recruitment, cell differentiation and restoration of multi-lineage hematopoiesis to avoid life-threatening complications.

PlGF enhances recruitment and migration of $VEGFR1^{+}$ HSCs

How does PlGF enhance early phases of hematopoietic recovery? PlGF increased mature WBC counts 2-fold above baseline, with a significant increase in circulating monocytes (Fig. 4*a*). Mobilization of hematopoietic cells into circulation followed the kinetics of PlGF plasma elevation (Fig. 4*a*, insert). Increased numbers of hematopoietic progenitors capable of forming CFU colonies (CFU-Cs) (Fig. 4*b*) were found within the PlGF-mobilized cells. PlGF augmented the number of circulating pluripotent hematopoietic cells (CFU-Ss) by 20-fold, as compared with controls three days after adenoviral injection (Fig. 4*c*). PlGF also mobilized $VEGFR1^{+}$ BM-repopulating stem cells that engrafted and rescued lethally irradiated recipients (Fig. 4*d*). More than 80% of BM-donor cells were detected in mice transplanted with PlGF-mobilized cells. We found that PlGF and VEGF-A stimulate the release of pro-MMP-9 (Fig. 4*e*, insert) and induce migration of human $CD34^{+}$ cells and cells with stem-cell potential (cobblestone-forming cells, CAFC). This migration was blocked by anti-VEGFR1 (Fig. 4*e*). These data suggest that PlGF is a chemoattractant that mediates its effect through VEGFR1, because blockade of VEGFR1 completely abolished HSC and progenitor mobilization *in vitro* and *in vivo*.

PlGF restores late phases of hematopoietic recovery

In the absence of exogenous growth factor(s), BM reconstitution is complete within 20–30 days following myelosuppression. Immediately post-BM suppression, quiescent $Lin^{-}Sca\text{-}1^{+}$ HSCs undergo rapid cell cycling to replenish the progenitor-cell pool. Blocking VEGFR1 signaling following myeloablation resulted in a decrease in immature $Sca\text{-}1^{+}$ and $Lin^{-}Sca\text{-}1^{+}$ BM cells in S phase of the cell cycle (Fig. 3*c, d* and *e*). *In vitro* exposure of $CD34^{+}$ cells to PlGF in the presence of sKitL, thrombopoietin and Flt3/Flk2 ligand had no effect on cell proliferation as determined by cell number, CFU-C and long-term culture-initiating cell assay (data not shown).

Therefore, the mechanism for the differential behavior of HSC *in vitro* and *in vivo* could be indirectly mediated through the release of a stem cell–active cytokine and/or through the activation of a protease regulating the bioavailability of cytokines. We demonstrate that PlGF induced matrix metalloproteinase-9 (MMP-9) expression in BM cells (Fig. 5*a*). If MMP-9

upregulation is the critical step during PlGF-mediated HSC mobilization, PlGF should not mobilize HSCs in MMP-9$^{-/-}$ mice. Indeed, plasma elevation of PlGF in wild-type, but not in MMP-9$^{-/-}$ mice, mobilized mature WBCs (Fig. 5*b*), CFU-Cs (Fig. 5*c*) and CFU-Ss (Fig. 5*d*), especially in later phases of PlGF-induced mobilization.

To confirm the role of PlGF-induced MMP-9 activation in BM recovery, we injected Ad-PlGF in 5FU-treated MMP-9$^{-/-}$ and MMP-9$^{+/+}$ mice. In the early phase of hematopoietic recovery, higher WBC counts were found in Ad-PlGF-treated mice, an MMP-9 independent process (Supplementary Fig. C online). In the late phase of hematopoietic recovery, Ad-PlGF improved WBC recovery in MMP-9$^{+/+}$, but not in MMP-9$^{-/-}$ mice. The improved WBC recovery in Ad-PlGF-treated MMP-9$^{-/-}$ mice translated into a slight reduction in the mortality following myelosuppression (Supplementary Fig. C online).

We recently showed that MMP-9-mediated release of soluble Kit-ligand (sKitL) is essential for hematopoietic reconstitution[4]. Notably, we detected a 10-fold increase in sKitL plasma levels in Ad-PlGF-treated mice as compared with controls (data not shown). PlGF-mediated MMP-9 activation is not critical during the early, but is necessary during the later phases of hematopoietic recovery following myelosuppression. As PlGF was not able to rescue 5FU-treated MMP-9$^{-/-}$ mice, we hypothesized that the late phases of BM recovery are indirectly regulated by PlGF-mediated release of sKitL. Therefore, if the release of sKitL after PlGF administration is mediated through MMP-9, significantly lower sKitL levels should be found in PlGF-treated MMP-9$^{-/-}$ as compared with MMP-9$^{+/+}$ mice, which was indeed the case (Fig. 5*e*). Because PlGF-mediated upregulation of MMP-9 augmented sKitL plasma levels, we predicted that administration of sKitL would rescue 5FU-myeloablated mice treated with anti-VEGFR1. Plasma elevation of sKitL restored survival (Fig. 6*a*), and hematopoietic recovery (Fig. 6*b–d*) of myeloablated mice treated with anti-VEGFR1. Remarkably, 5FU-treated mice injected with neutralizing anti-VEGFR1 showed significantly decreased sKitL plasma levels as compared with VEGFR2-treated or control mice (Fig. 6*e*). These data suggest that during late phases of BM recovery PlGF-mediated upregulation of MMP-9 facilitates the release of sKitL, thereby promoting cell differentiation and accelerates hematopoietic reconstitution (Fig. 6*f*).

Discussion

We demonstrate here that human and murine HSCs with long-term BM-repopulating capacity express VEGFR1, conveying signals regulating cell cycling and motility. Inhibition of VEGFR1, but not VEGFR2, blocked recruitment of HSCs from their resting microenvironment, thereby retarding hematopoietic reconstitution after myelosuppression. PlGF augmented early phases of hematopoietic recovery by promoting recruitment, chemotaxis and mobilization of VEGFR1^{+} HSCs and progenitors, while during late phases of BM recovery PlGF-mediated upregulation of MMP-9 facilitated the release of sKitL thereby accelerating hematopoietic reconstitution.

Our data suggest that PlGF activates non-angiogenic pathways and thus serves functions other than regulating angiogenesis. Based on our data, the accumulation of angioblasts within the yolk sac in VEGFR1$^{-/-}$ mice may not only be due to enhanced commitment to angioblasts[17], but may be due to impaired cell migration. This appears to be the case in *Drosophila*, where VEGF-A activation is directly linked to hemocyte motility[23].

How does VEGFR1 activation increase HSC motogenic potential? Chemotaxis of VEGFR1^{+} HSCs and progenitors accounts for the WBC increase in the early phase of PlGF mobilization. PlGF mobilized CFU-Cs and CFU-Ss in MMP-9$^{+/+}$, but to a lesser extent in MMP-9$^{-/-}$ mice. In later phases, PlGF-induced cell mobilization was impaired in MMP-9$^{-/-}$

mice, suggesting that PlGF recruits HSCs and progenitors by a different mechanism. PlGF induces the release of sKitL through MMP-9 activation. sKitL increases motility by promoting cell cycle transition through interaction with its receptor c-Kit[29,30]. Activation of this pathway accounts for the hematopoietic reconstitution during later phases of BM recovery. Indeed, neutralizing anti-VEGFR1 profoundly diminished plasma elevation of sKitL in myelosuppressed mice during BM recovery, while introduction of sKitL into myelosuppressed mice treated with anti-VEGFR1 completely restored hematopoiesis.

The increase in cell cycling and proliferation of VEGFR1$^+$Sca-1$^+$ cells after BM suppression is most likely not a direct effect of PlGF, because activation of VEGFR1 did not change HSC survival or colony formation *in vitro*. These data support other reports in which VEGF-A or PlGF had no major effect on the proliferation or survival of HSCs or progenitors[31–33]. However, these studies do not rule out the possibility that VEGF/VEGFR internal autocrine signaling pathways may synergize with other cytokines to convey survival signals for repopulating cells.

Although VEGFR2 is expressed on human NOD/SCID-repopulating cells[14], the functional role of VEGFR2 in the regulation of post-natal hematopoiesis remains unclear. Transplantation of murine VEGFR2$^+$ BM cells failed to reconstitute hematopoiesis in lethally irradiated recipients[15]. These data suggest that murine BM-derived VEGFR2$^+$ cells may mark endothelial progenitors[1,34] rather than repopulating HSCs. Supporting these observations, we showed only a transient delay in the recovery of lymphoid and erythroid precursors in mice treated with neutralizing anti-VEGFR2. This delay in hematopoietic recovery was not sufficient to induce life-threatening complications, since all mice treated with 5FU and anti-VEGFR2 survived. Anti-VEGFR2 may delay the recovery of certain lineages through interference with the production of lineage-specific cytokines, such as GM-CSF and IL-6 (ref. [35]).

In contrast, mice treated with 5FU and neutralizing anti-VEGFR1 showed a striking impaired tri-lineage cell recovery with prolonged pancytopenia, which resulted in the demise of 70% of treated mice kept under germ-free conditions. The lack of a more profound defect in myelosuppressed mice treated with anti-VEGFR2 seems to be in disagreement with the dramatic defect in blood-island formation observed in VEGFR2-null mice. It is difficult to compare the role of VEGFR2 signaling in the regulation of hematopoiesis in the embryo and adult mice, as there are fundamental differences between the established post-natal BM microenvironment and fragile embryonic blood islands. Adult BM stromal cells provide a fortified cellular scaffold that may be resistant to effects of anti-VEGFR2. Since stromal cells express VEGFR1[36], it is conceivable that anti-VEGFR1 block MMP-9 expression leading to failure of the recruitment of HSCs. This may explain why anti-VEGFR1 compromises hematopoietic recovery, while inhibition of VEGFR2 has only a marginal effect on stress hematopoiesis.

We have shown that plasma elevation of $VEGF_{165}$ with or without angiopoietin-1 promoted mobilization of HSCs and CFU-Cs (ref. [22]). Here, we show that, under steady-state conditions, chronic inhibition of VEGFR1 or VEGFR2 had no major effect on hematopoiesis. This is in sharp contrast to the failure of hematopoietic reconstitution and demise of the treated mice by inhibiting VEGFR1 during BM suppression. These data suggest that during steady-state hematopoiesis, VEGFR1 inhibition does not result in a profound impairment in hematopoiesis, because the demand for HSC recruitment is low. In contrast, during stress hematopoiesis activation of VEGFR1 is necessary for hematopoietic reconstitution. This phenomenon is similar to other physiological processes requiring rapid tissue vascularization, where stress angiogenesis driven by the mobilization of VEGFR2$^+$ BM-derived cells is necessary to accelerate neo-angiogenesis[1]. These data suggest that in stress hematopoiesis the molecular

switch requires activation of VEGFR1, whereas during stress angiogenesis the molecular switch is driven by VEGFR2 activation.

Based on our data, the clinical use of VEGFR1 inhibitors, but to a lesser degree VEGFR2, delivered in combination with myelosuppressive agents, may result in a life-threatening prolongation of BM suppression. In this respect, suppression of hematopoiesis through VEGFR1 inhibition has two ramifications. On one hand, blocking VEGFR1 may inhibit tumor angiogenesis and growth, but on the other hand, it may introduce unwanted BM toxicity. Nonetheless, since VEGFR1 toxicity is dose-dependent, VEGFR1 inhibitors can be delivered with a manageable toxicity profile. Simultaneous administration of sKitL may reduce BM toxicity caused by blocking VEGFR1 and therefore rescue patients from infection or hemorrhage.

Stress promotes mobilization of BM-derived stem cells that ultimately incorporate, although at very low levels, into specific organs. This low efficiency of incorporation may be reflected in the paucity of readily motile stem cells capable of being recruited from the BM to circulation. PlGF, endowed with a low toxicity profile, allows for mobilization of stem cells to the circulation, facilitating recovery of many stem cells that may ultimately be used for organ restoration.

Our findings introduce the novel paradigm that determination of VEGFR1 and MMP-9 expression should be considered as surrogate markers for evaluating the efficacy and success of stem cell mobilization and engraftment in transplantation settings. It is conceivable that dysregulated MMP-9, VEGFR1 or PlGF expression may be responsible for defects in the stem-cell microenvironment leading to BM failure. In this regard, therapeutic strategies to upregulate VEGFR1, PlGF and MMP-9 may provide an effective means to restore motogenic potential of BM-repopulating cells and help to replenish the stem cell pool after BM transplantation.

Methods

Animals

BALB/c, C57BL/6Ly5.1, C57BL/6Ly5.2 and NOD/SCID mice, from the Jackson Laboratory (Bar Harbor, Maine) and MMP-$9^{-/-}$ and MMP-$9^{+/+}$ 129Sv mice (used after >8 back crosses to CD1)[37], age- and sex-matched (7–8 wk), weight (>20 g) were maintained in Thorensten units. Animal experiments were performed with approval and authorization of the institutional review board and the Animal Care and Use Committee of Cornell University Medical College, Sloan-Kettering Institute and the UCSF Committee on Animal Research.

Antibodies

Murine cells were stained with the following monoclonal antibodies from PharMingen (San Diego, California): anti-B220 (RA3-6B2), Sca-1 (E13.161.7 and D7), Gr-1, TER119 (TER-119), Thy1.2 (53-2.1), CD11b (M1/70), CD41 (MWReg30), CD45 (30.F11), Ly5.1 (A20), Ly5.2 (104). c-Kit (2B8) was purchased from Biosciences. Rat neutralizing antibody against mouse VEGFR1 and VEGFR2 (MF-1, DC101, respectively)[10,38] and mouse antibody against human VEGFR1 FB5) were developed by ImClone Systems (New York, New York) [35,39–41]. Murine VEGFR1 antibody was biotinylated or labeled with Cy2.

Cell isolation

For murine $Lin^{-}Sca\text{-}1^{+}$ cells, lineage-negative BM cells (Lin^{-}) were isolated with magnetic beads (Miltenyi Biotec) using a cocktail of lineage-specific antibodies (Stem Cell Technology, Vancouver, Canada). Lin^{-} cells were further labeled with Sca-1 magnetic beads and MACS separated (Miltenyi Biotec). $Lin^{-}Sca\text{-}1^{+}$ BM cells were >95% positive for Sca-1 and Thy1.

For murine VEGFR1$^+$ cells, BALB/c mice were injected with 5FU (150 mg/kg, Pharmacia, Albuquerque, New Mexico) intravenously (i.v.). BMMCs were labeled with biotinylated murine VEGFR1 and Avidin magnetic beads (Miltenyi Biotec) and separated using MACS. Purity of VEGFR1$^+$ BMMCs was >92–98%.

Transplantation

For the NOD/SCID repopulating assay, sublethaly irradiated (3.5Gy) NOD/SCID mice were transplanted with serial doses of MACS-isolated CD34$^+$, CD34$^+$VEGFR1$^+$ and CD34$^+$VEGFR$^-$ cells. Purity of different subsets was >97%. To determine human/mouse chimerism, BMMCs were stained with murine CD45-FITC and human CD45-PE (PharMingen, San Diego, California).

To assess the long-term repopulating capacity of VEGFR1$^+$ cells, 15 male BALB/c mice were injected i.v. with 5FU (150 mg/kg) 2 d before BMMCs collection. Female recipients (n = 10 per group) were lethally irradiated (9 Gy) and i.v. injected with serial cell doses of MACS-isolated VEGFR1$^+$ or VEGFR1$^-$ BMMCs on day 0.

To assess the long -term repopulating capacity of VEGFR1$^{+/-}$ Sca-1$^{+/-}$ cells, 2 d after collecting BMMCs from fifteen 5FU-treated (150 mg/kg) C57BL/6Ly5.2 mice, VEGFR1$^{+/-}$ and Sca-1$^{+/-}$ BMMCs were separated using a MoFlo cell sorter. VEGFR1$^+$ or VEGFR1$^-$ cells were transplanted into lethally irradiated C57BL/6Ly5.1 mice (n = 12 per group).

For the CFU-S assay, mobilized PBMCs (1×10^5 per mouse) of PlGF-treated mice were injected i.v. into lethally irradiated syngeneic recipients (9 Gy) as described[4].

In vivo antibody-blocking experiments

5FU-treated (300 mg/kg) BALB/c mice were co-injected intraperitoneally with 800 μg anti-mouse VEGFR1 (clone MF-1), anti-mouse VEGFR2 (clone DC101) or IgG as a control at 2-day intervals starting day 0. Anti-mouse VEGFR1 at 1 μg/ml blocked >90% of PlGF-mediated and >50% of VEGF-mediated activity *in vitro*.

Cytokine administration

Plasma PlGF and sKitL levels were elevated using a single injection of adenovirus (Ad) vector[22,42]. Mice received Ad-vector expressing human PlGF (Ad-PlGF) or no transgene (Ad-null) at a concentration of 1×10^9 plaque-forming units (p.f.u.) and Ad-vector expressing sKitL (AdsKitL) at a concentration of 1.5×10^8 p.f.u. Recombinant G-CSF (R&D Systems) was administered s.c. daily from day 0–14 (50 μg/kg).

Myelosuppressive regiments

Mice received a single i.v. injection of 5FU (300 mg/kg) or carboplatin (1.2 mg) plus total body irradiation (5 Gy) on day 0.

Peripheral blood analysis

Blood was collected from mice by retro-orbital bleeding. WBC and granulocytes counts were determined. Wright/Giemsa-stained blood smears were analyzed for the presence of monocytes. Plasma samples were collected, and human PlGF and murine sKitL (SCF) measured using an ELISA (R&D Systems, Minneapolis, Minnesota). PBMCs were isolated from heparinized blood after centrifugation over a discontinuous gradient using Lympholyte-M (Cedarlane, Ontario, Canada).

Colony-forming assay

PBMCs (1×10^5) were plated in a methylcellulose-based colony assay including murine sKitL, IL-3 and human erythropoietin[4]. Colonies were scored after 7 d.

Cell-cycle analysis

BMMCs of 5FU-injected BALB/c mice treated with neutralizing anti-VEGFR1, anti-VEGFR2 or IgG *in vivo* were labeled with Sca-1-FITC. $Lin^-Sca\text{-}1^+$ BM cells (purity >95% for Sca-1 and Thy1.2) were stained for VEGFR1-Cy2. $Sca\text{-}1^+/Lin^-Sca\text{-}1^+VEGFR1^+$ BM cells were fixed in ice-cold ethanol. After RNase treatment (Sigma), cells were stained with propidium iodide (Molecular-Probes, Eugene, Oregon). DNA content of $Sca\text{-}1^+$ and $VEGFR1^+$ cells was determined by FACS.

FISH analysis

4 mo after transplantation, male donor BMMCs were detected in female recipients using the murine Y-chromosome-specific probe M34.

Immunohistochemistry

Sections were incubated with MMP-9 antibody (clone 7-11C, Oncogene, Boston, Massachusetts), biotinylated horse anti-mouse IgG and A&B reagents (Vector) and the M.O.M. kit (Vector, Burlingame, California) was used. Sections were stained with anti-human vWF/HRP (Dako). Sections were developed with 3,3′-diaminobenzidine substrate and counterstained with eosin or hematoxylin.

In vitro transmigration

Human $CD34^+$ cells (purity>95%) were added to 8-μm-pore Matrigel-coated transwell inserts (Costar, Cambridge, Massachusetts). Recombinant PlGF (R&D Systems; 100 ng/ml) or VEGF-A (R&D Systems; 100 ng/ml) was added to the lower chamber with/without neutralizing anti-VEGFR1 (1μg/ml), which was added to both chambers. Transmigrated cells were placed in cultures to measure the number of CFU-C and CAFC (ref. [4]).

Statistical analysis

Results are expressed as mean ± s.e.m. Data were analyzed using the unpaired two-tailed Student's *t*-test and the log-rank test. $P < 0.05$ was considered significant.

Supplementary Material

Refer to Web version on PubMed Central for supplementary material.

Acknowledgments

This work was supported by grants from the National Heart, Lung, and Blood Institute R01s, HL-58707, HL-61849, HL-66592, HL-67839 (to S.R.); the American Cancer Society (to S.R.); Leukemia and Lymphoma Foundation (to S.R.); the Doris Duke Charitable Foundation (to D.L.); National Institutes of Health, CA 72006, CA 75072, NS39278 and AR46238 (to Z.W.), and National Institutes of Health R01 HL61401 (to MASM).

References

1. Lyden D, et al. Impaired recruitment of bone-marrow-derived endothelial and hematopoietic precursor cells blocks tumor angiogenesis and growth. Nature Med 2001;7:1194–1201. [PubMed: 11689883]
2. Cheng T, et al. Hematopoietic stem cell quiescence maintained by p21cip1/waf1. Science 2000;287:1804–1808. [PubMed: 10710306]

3. Peled A, et al. Dependence of human stem cell engraftment and repopulation of NOD/SCID mice on CXCR4. Science 1999;283:845–851. [PubMed: 9933168]
4. Heissig B, et al. Recruitment of stem cells from bone marrow niche requires MMP-9 mediated release of Kit ligand. Cell 2002;109:625–637. [PubMed: 12062105]
5. Berardi AC, Wang A, Levine JD, Lopez P, Scadden DT. Functional isolation and characterization of human hematopoietic stem cells. Science 1995;267:104–108. [PubMed: 7528940]
6. Phillips RL, et al. The genetic program of hematopoietic stem cells. Science 2000;288:1635–1640. [PubMed: 10834841]
7. Krause DS, et al. Multi-organ, multi-lineage engraftment by a single bone marrow-derived stem cell. Cell 2001;105:369–377. [PubMed: 11348593]
8. Carmeliet P, Jain RK. Angiogenesis in cancer and other diseases. Nature 2000;407:249–257. [PubMed: 11001068]
9. Hanahan D, Folkman J. Patterns and emerging mechanisms of the angiogenic switch during tumorigenesis. Cell 1996;86:353–364. [PubMed: 8756718]
10. Carmeliet P, et al. Synergism between vascular endothelial growth factor and placental growth factor contributes to angiogenesis and plasma extravasation in pathological conditions. Nature Med 2001;7:575–583. [PubMed: 11329059]
11. Kabrun N, et al. Flk-1 expression defines a population of early embryonic hematopoietic precursors. Development 1997;124:2039–2048. [PubMed: 9169850]
12. Shalaby F, et al. Failure of blood-island formation and vasculogenesis in Flk-1-deficient mice. Nature 1995;376:62–66. [PubMed: 7596435]
13. Shalaby F, et al. A requirement for Flk1 in primitive and definitive hematopoiesis and vasculogenesis. Cell 1997;89:981–990. [PubMed: 9200616]
14. Ziegler BL, et al. KDR receptor: A key marker defining hematopoietic stem cells. Science 1999;285:1553–1558. [PubMed: 10477517]
15. Haruta H, Nagata Y, Todokoro K. Role of Flk-1 in mouse hematopoietic stem cells. FEBS Lett 2001;507:45–48. [PubMed: 11682057]
16. Fong GH, Rossant J, Gertsenstein M, Breitman ML. Role of the Flt-1 receptor tyrosine kinase in regulating the assembly of vascular endothelium. Nature 1995;376:66–70. [PubMed: 7596436]
17. Fong GH, Zhang L, Bryce DM, Peng J. Increased hemangioblast commitment, not vascular disorganization, is the primary defect in flt-1 knock-out mice. Development 1999;126:3015–3025. [PubMed: 10357944]
18. Hiratsuka S, et al. Involvement of Flt-1 tyrosine kinase (vascular endothelial growth factor receptor-1) in pathological angiogenesis. Cancer Res 2001;61:1207–1213. [PubMed: 11221852]
19. Sawano A, et al. Flt-1, vascular endothelial growth factor receptor 1, is a novel cell surface marker for the lineage of monocyte-macrophages in humans. Blood 2001;97:785–791. [PubMed: 11157498]
20. Clauss M, et al. The vascular endothelial growth factor receptor Flt-1 mediates biological activities. Implications for a functional role of placenta growth factor in monocyte activation and chemotaxis. J Biol Chem 1996;271:17629–17634. [PubMed: 8663424]
21. Barleon B, et al. Migration of human monocytes in response to vascular endothelial growth factor (VEGF) is mediated via the VEGF receptor flt-1. Blood 1996;87:3336–3343. [PubMed: 8605350]
22. Hattori K, et al. Vascular endothelial growth factor and angiopoietin-1 stimulate postnatal hematopoiesis by recruitment of vasculogenic and hematopoietic stem cells. J Exp Med 2001;193:1005–1014. [PubMed: 11342585]
23. Cho NK, et al. Developmental control of blood cell migration by the *Drosophila* VEGF pathway. Cell 2002;108:865–876. [PubMed: 11955438]
24. Van Zant G. Studies of hematopoietic stem cells spared by 5-fluorouracil. J Exp Med 1984;159:679–690. [PubMed: 6699542]
25. Randall TD, Weissman IL. Phenotypic and functional changes induced at the clonal level in hematopoietic stem cells after 5-fluorouracil treatment. Blood 1997;89:3596–3606. [PubMed: 9160664]

26. Goodell MA, et al. Dye efflux studies suggest that hematopoietic stem cells expressing low or undetectable levels of CD34 antigen exist in multiple species. Nature Med 1997;3:1337–1345. [PubMed: 9396603]
27. Briddell RA, Hartley CA, Smith KA, McNiece IK. Recombinant rat stem cell factor synergizes with recombinant human granulocyte colony-stimulating factor *in vivo* in mice to mobilize peripheral blood progenitor cells that have enhanced repopulating potential. Blood 1993;82:1720–1723. [PubMed: 7691233]
28. Laterveer L, et al. Interleukin-8 induces rapid mobilization of hematopoietic stem cells with radioprotective capacity and long-term myelolymphoid repopulating ability. Blood 1995;85:2269–2275. [PubMed: 7718900]
29. Morrison SJ, et al. Identification of a lineage of multipotent hematopoietic progenitors. Development 1997;124:1929–1939. [PubMed: 9169840]
30. Morrison SJ, Wright DE, Weissman IL. Cyclophosphamide/granulocyte colony-stimulating factor induces hematopoietic stem cells to proliferate prior to mobilization. Proc Natl Acad Sci USA 1997;94:1908–1913. [PubMed: 9050878]
31. Huang XL, Takakura N, Suda T. *In vitro* effects of angiopoietins and VEGF on hematopoietic and endothelial cells. Biochem Biophys Res Commun 1999;264:133–138. [PubMed: 10527853]
32. Broxmeyer HE, et al. Myeloid progenitor cell regulatory effects of vascular endothelial cell growth factor. Int J Hematol 1995;62:203–215. [PubMed: 8589366]
33. Ratajczak MZ, et al. Role of vascular endothelial growth factor (VEGF) and placenta-derived growth factor (PlGF) in regulating human haemopoietic cell growth. Br J Haematol 1998;103:969–979. [PubMed: 9886308]
34. Peichev M, et al. Expression of VEGFR-2 and AC133 by circulating human CD34(+) cells identifies a population of functional endothelial precursors. Blood 2000;95:952–958. [PubMed: 10648408]
35. Dias S, et al. Inhibition of both paracrine and autocrine VEGF/VEGFR-2 signaling pathways is essential to induce long-term remission of xenotransplanted human leukemias. Proc Natl Acad Sci USA 2001;98:10857–10862. [PubMed: 11553814]
36. Gerber HP, et al. VEGF couples hypertrophic cartilage remodeling, ossification and angiogenesis during endochondral bone formation. Nature Med 1999;5:623–628. [PubMed: 10371499]
37. Vu TH, et al. MMP-9/gelatinase B is a key regulator of growth plate angiogenesis and apoptosis of hypertrophic chondrocytes. Cell 1998;93:411–422. [PubMed: 9590175]
38. Prewett M, et al. Antivascular endothelial growth factor receptor (fetal liver kinase 1) monoclonal antibody inhibits tumor angiogenesis and growth of several mouse and human tumors. Cancer Res 1999;59:5209–52018. [PubMed: 10537299]
39. Zhu Z, et al. Inhibition of vascular endothelial growth factor-induced receptor activation with anti-kinase insert domain-containing receptor single-chain antibodies from a phage display library. Cancer Res 1998;58:3209–3214. [PubMed: 9699643]
40. Zhu Z, et al. Inhibition of vascular endothelial growth factor induced mitogenesis of human endothelial cells by a chimeric anti-kinase insert domain- containing receptor antibody. Cancer Lett 1999;136:203–213. [PubMed: 10355750]
41. Witte L, et al. Monoclonal antibodies targeting the VEGF receptor-2 (Flk1/KDR) as an anti-angiogenic therapeutic strategy. Cancer Metastasis Rev 1998;17:155–161. [PubMed: 9770111]
42. Hattori K, et al. Plasma elevation of stromal cell-derived factor-1 induces mobilization of mature and immature hematopoietic progenitor and stem cells. Blood 2001;97:3354–3360. [PubMed: 11369624]

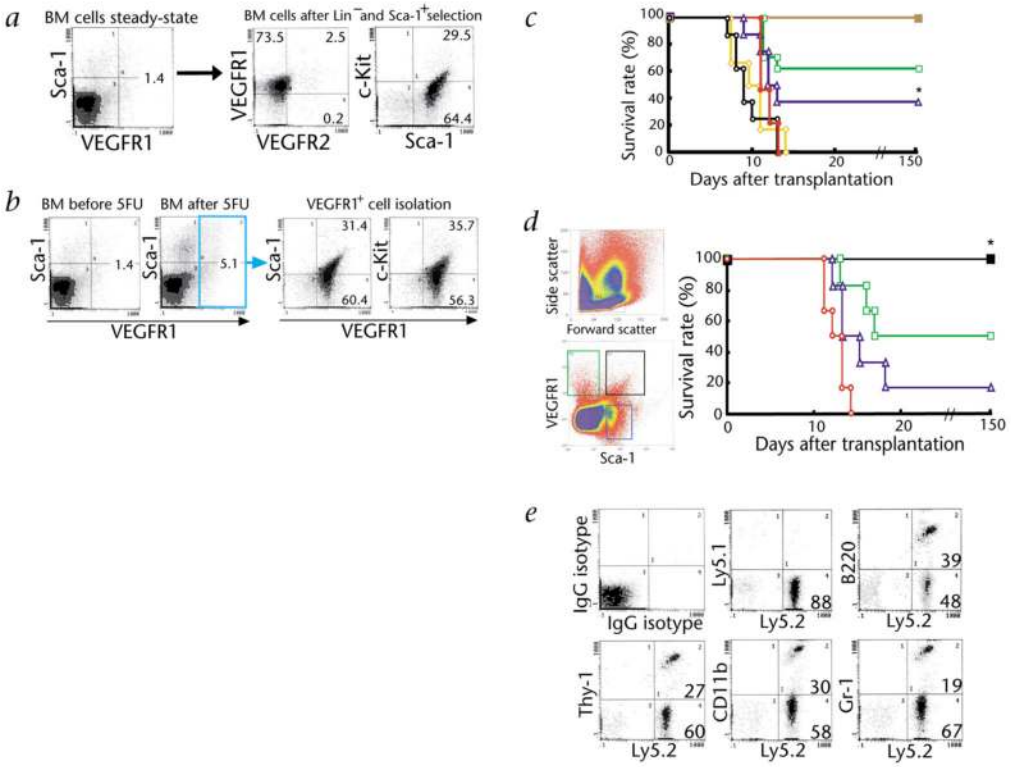

Fig. 1.

VEGFR1 is expressed on pluripotent murine HSCs with short-and long-term repopulating capacity. ***a***, Unseparated and MACS-isolated Lin^{-}Sca-1^{+} BM cells from BALB/c mice were stained for VEGFR1-Cy2, Sca-1-FITC and PE-conjugated antibody to Sca-1, c-Kit and VEGFR2 and analyzed by FACS. ***b*** and ***c***, BM cells were collected 2 d after BALB/c mice had received 5FU i.v. for HSCs enrichment[24,25]. *b*, Isolated VEGFR1 BMMCs were stained with Cy2-conjugated anti-VEGFR1, with PE-conjugated anti-Sca-1 and c-Kit and were analyzed by FACS. Representative percentages of positive populations in BMMCs are shown ($n = 6$). *c*, Lethally irradiated female mice were transplanted with serial doses of MACS-isolated syngeneic male VEGFR1^{+} BMMCs. ■, 1×10^5; □, 1×10^3; △, 1×10^2; ◇, 1×10^1 VEGFR1^{+} BMMCs. ○, 1×10^5 VEGFR1^{-} BMMCs. ●, 1×10^5 VEGFR2^{+} BMMCs. Mice transplanted with 1×10^2 VEGFR1^{+} BMMCs showed improved survival versus mice transplanted with 1×10^5 VEGFR1^{-} BMMCs or VEGFR2^{+} BMMCs ($n = 10$; *, $P < 0.05$). ***d*** and ***e***, BM cells obtained from 5FU-treated C57BL/6-Ly5.2 mice were stained for VEGFR1-Cy2 and Sca-1-PE. Singly and doubly positive VEGFR1/Sca-1 BM cells (1×10^3) isolated by MoFlo cell sorter were transplanted into lethally irradiated C57BL/6-Ly5.1 mice. ■, VEGFR1^{+}Sca-1^{+}; □, VEGFR1^{+}Sca-1^{-}; △, VEGFR1^{-}Sca-1^{+}; ○, VEGFR1^{-}Sca-1^{-} of BM cells. *d*, Survival rate was improved in mice transplanted with 1×10^3 VEGFR1^{+}Sca-1^{-} cells compared with mice transplanted with VEGFR1^{-}Sca-1^{+} cells ($n = 12$; *, $P < 0.05$). *e*, 5 mo after transplantation, the percentage of donor (Ly5.2)-derived myeloid (CD11b and Gr-1) and lymphoid (Thy-1 and B220) cells in the peripheral blood of recipient mice (Ly5.1) was analyzed by FACS. A representative FACS analysis is shown in which 88.3% chimerism was achieved 150 d after transplantation.

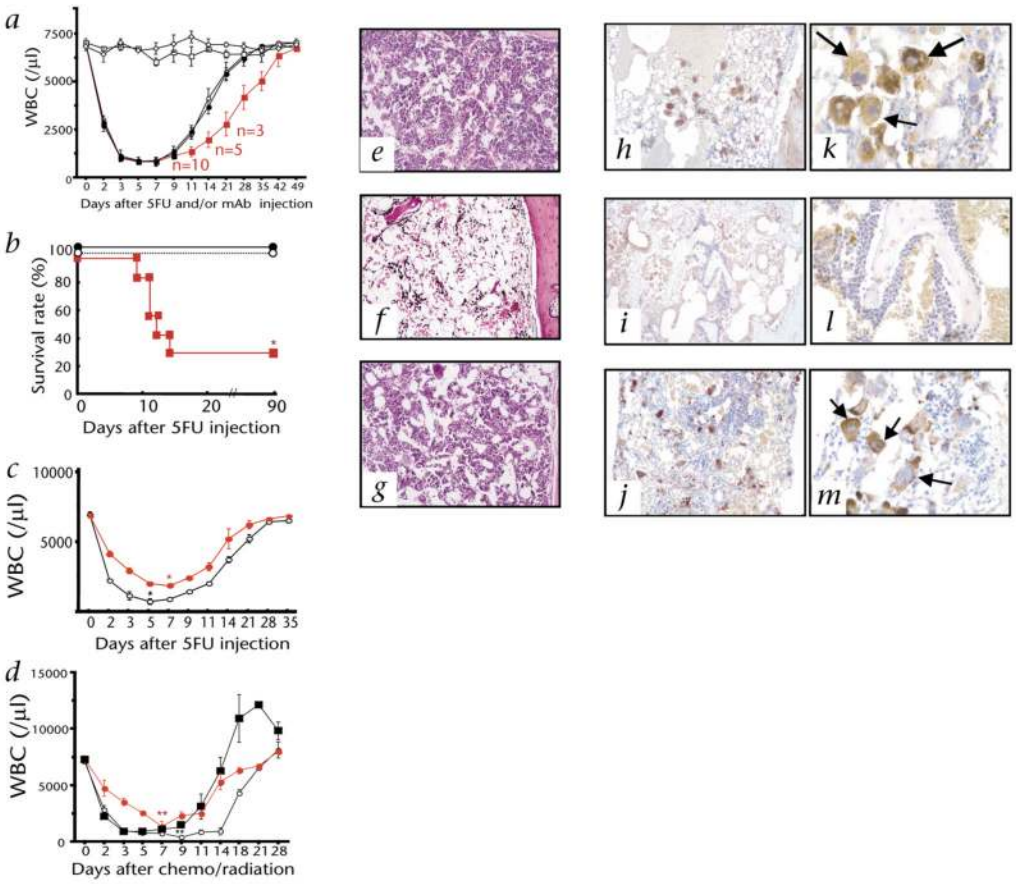

Fig. 2.

Inhibition of VEGFR1, but not VEGFR2, after myelosuppression, results in delayed hematopoietic recovery and increased mortality of the treated mice. ***a*** and ***b***, Myelosuppression was induced by a single dose of 5FU. 12 5FU-treated BALB/c mice in each group were injected i.p. with neutralizing doses of anti-VEGFR1 (■), anti-VEGFR2 (●) or IgG control (○) in 2-d intervals starting from day 0. Mice were also treated with anti-VEGFR1 (□) and anti-VEGFR2 (◇) alone. *a*, WBCs were quantified. *b*, Survival rate was monitored on a daily basis. Survival rate was lower in the VEGFR1-treated versus IgG-treated mice (*, $P < 0.001$). ***c*** and ***d***, Hematopoietic recovery following a single dose of 5FU on day 0 (*c*) or total body irradiation (TBI) plus carboplatin at day 0 (*d*) ($n = 6$ for both) followed by a single dose of either Ad-PlGF (●) or Ad-null (○) on day 0. *d*, Recombinant G-CSF (injected subcutaneously day 0–14, ■) promotes rapid hematopoietic reconstitution. Extent and duration of less than 2000/μl WBCs was significantly shorter in the Ad-PlGF-treated versus Ad-null-treated 5FU- and carboplatin/irradiation-treated mice. *c*, *, $P < 0.001$; *d*, *, $P < 0.005$. Error bars represent mean ± s.e.m. for 6–10 mice per group. ***e–g***, H&E staining of BM sections of 5FU-treated mice 10 d after co-injection with neutralizing anti-VEGFR1 (*f*), anti-VEGFR2 (*g*) or IgG controls (*e*). Magnification, × 100. ***h–m***, vWF staining of BM sections 10 d after 5FU treatment in antibody-treated mice (anti-VEGFR1 (*i* and *l*), anti-VEGFR2 (*j* and *m*) or IgG controls (*h* and *k*); megakaryocytes are depicted by arrows). Magnifications, ×100 (*h–j*); ×400 (*k–m*).

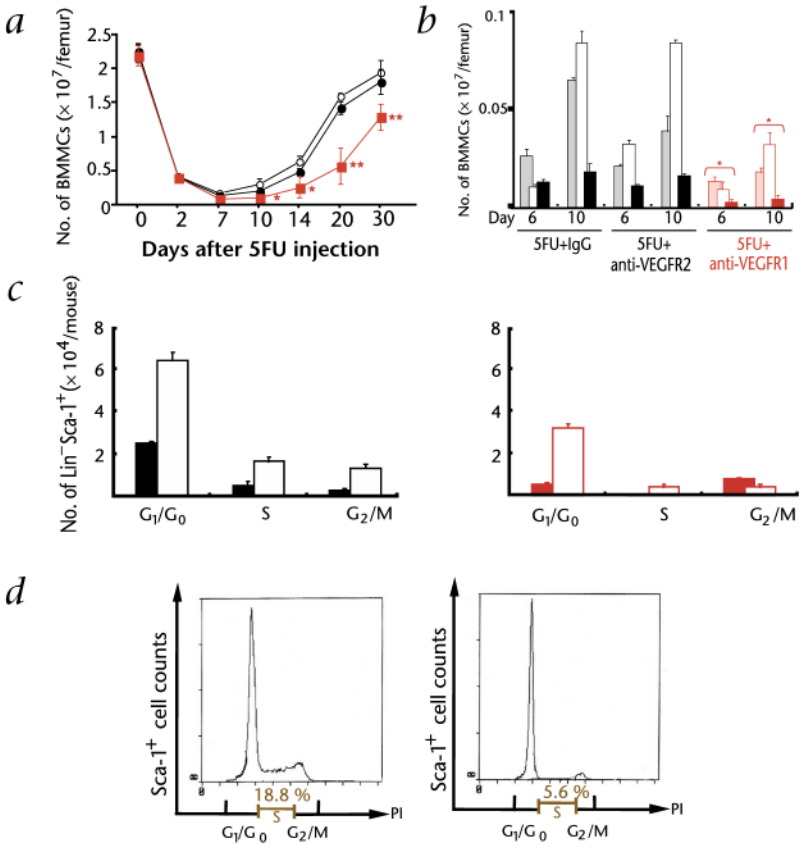

	5FU + IgG			5FU+ anti-VEGFR1		
Day	G_1/G_0	S	G_2/M	G_1/G_0	S	G_2/M
6	74.2 ± 5.1	14.9 ± 3.9	8.8 ± 2.2	83.3 ± 2.9	6.0 ± 1.0*	7.2 ± 1.1
8	68.4 ± 2.3	17.7 ± 2.2	12.4 ± 0.9	82.1 ± 1.0	7.5 ± 0.9*	7.3 ± 1.0*
10	64.3 ± 4.7	19.5 ± 4.0	14.4 ± 0.7	80.0 ± 1.2	9.4 ± 0.3*	8.4 ± 0.8*

Fig. 3.

Blocking VEGFR1 signaling after myeloablation inhibits cell-cycle progression, proliferation and differentiation of HSCs. ***a***, Mice received a myeloablative dose of 5FU by a single injection on day 0 ($n = 9$ per group). Mice were co-injected i.p. with neutralizing antibodies to VEGFR1 (■), VEGFR2 (●) or IgG controls (○) in 2-day intervals. 3 mice treated with anti-VEGFR1 or anti-IgG were killed at each time point. Quantification of total BMMCs obtained from BM of treated and untreated mice (*, $P < 0.05$; **, $P < 0.01$). ***b***, BMMCs were stained with different lineage-restricted antigens including the B cell–associated antigen B220 (shaded bar), the myeloid marker CD11b (empty bar) and the erythroid marker TER119 (filled bar). *, $P < 0.05$ for absolute number of lineage-derived cells in the anti-VEGFR1-treated versus the control groups. ***c***, Cell cycle of $Lin^-Sca\text{-}1^+VEGFR1^+$ cells, after 5FU treatment, was determined after staining of $Lin^-Sca\text{-}1^+$ cells with VEGFR1-Cy2 and propidium iodide on day 6 (■) and day 10 (□) after 5FU + IgG (left) and 5FU + anti-VEGFR1(right). DNA content was quantified and assessed by flow cytometry. Absolute number of cells in different phases of the cell cycle is given. ***d*** and ***e***, Cell cycle of $Sca\text{-}1^+$ BMMCs, after 5FU treatment, was determined by staining with Sca-1-FITC and propidium iodide. Representative data from day 6 are shown as

histograms with IgG (left) and anti-VEGFR1 (right) (*d*). Percentage of Sca-1$^+$ cells in the S and G_2/M phase from anti-VEGFR1-treated versus IgG-treated control group (*e*). *, $P < 0.001$. Error bars represent mean ± s.e.m. for 9 mice per group (*a*) or for 3 independent experiments (*b*, *c*, and *e*).

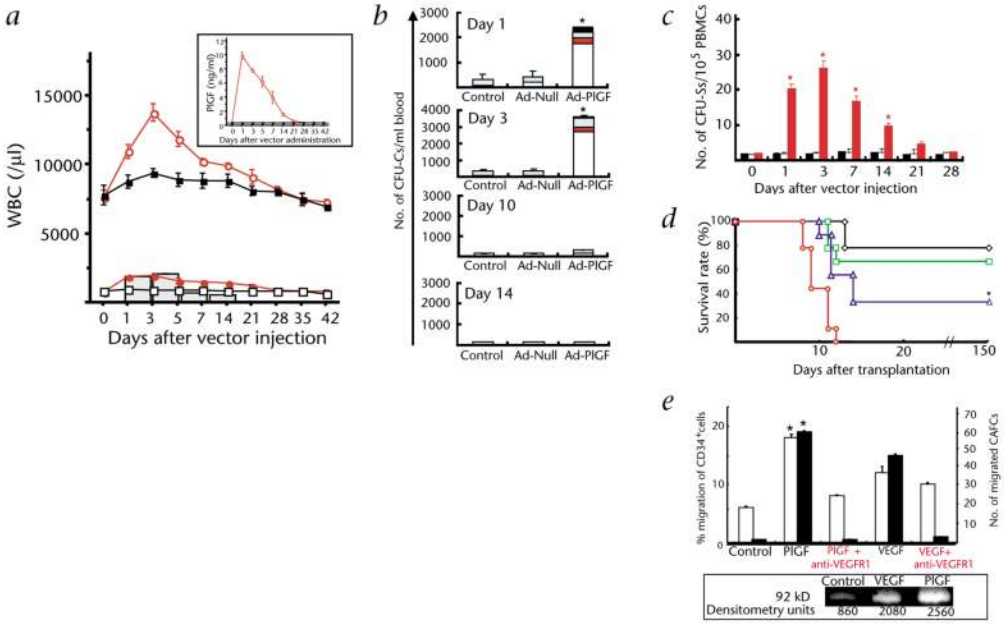

Fig. 4.

PlGF augments motogenic potential of VEGFR1$^+$ BM-repopulating stem and progenitor cells. ***a,*** BALB/c mice received Ad-PlGF or Ad-null vector by a single i.v. injection on day 0 (n = 6). *a*, Total WBCs, monocytes (bar graph) and neutrophil cell counts were quantified. ○, WBCs in Ad-PlGF-treated group; ■, WBCs in Ad-null-treated group; ●, neutrophils in Ad-PlGF-treated group; (□), neutrophils in Ad-null-treated group. Plasma PlGF levels after adenovirus administration were measured by ELISA (insert). ***b***, Number of mobilized progenitors was quantified by using CFU assays. As compared with Ad-null controls, there was a 14-fold increase in the number of circulating progenitors in Ad-PlGF-treated mice. □, CFU-GM; ■, CFU-GEMM; ■, CFU-M; ■, BFU-E. (n = 6; *, $P < 0.001$). ***c*** and ***d***, Pluripotency of mobilized cells was assessed by CFU-S assay (*c*) and BM repopulating assay (*d*). *c*, Mobilized PBMCs from Ad-PlGF (■), Ad-null (□) and control mice (■) were injected into lethally irradiated recipient mice and spleens were harvested on day 12. CFU-S were counted (*, $P < 0.001$). *d*, PBMCs obtained from male donor mice were collected 1 d after treatment with Ad-null and Ad-PlGF vectors. PBMCs of Ad-PlGF-treated mice (◇, 1×10^6; □, 5×10^5; △, 1×10^5; ○, 5×10^4 cells) and Ad-null-treated mice were transplanted into lethally irradiated female recipients (n = 12 per group). In mice injected with as low as 1×10^5 PlGF-mobilized PBMC cells, there was a significant improvement in survival of recipient mice versus mice transplanted with Ad-null-derived PBMCs (*, $P < 0.05$). ***e***, Human CD34$^+$ cells were plated in Matrigel-coated transwells. The chemoat-tractants PlGF or VEGF were added to the lower chamber, while anti-VEGFR1 was added to both chambers. Data are shown as a percentage of migrated cells (□). Migrated cells with stem cell potential were quantified by the capacity of cobblestone formation on wk 5, (CAFC wk 5; ■) (n = 3; *, $P < 0.001$ for migration towards chemoattractant PlGF of cells treated with/without anti-VEGFR1). Bottom, Gelatin zymogram of supernatants from human CD34$^+$ cells stimulated with or without PlGF or VEGF in serum-free medium. Supernatants from CD34$^+$-cell cultures showed gelatinolytic activity for pro-MMP-9 (92 kD). Error bars represent mean ± s.e.m. for 6 mice per experimental condition (*a*), and 3 independent experiments (*b*, *c*, *e*).

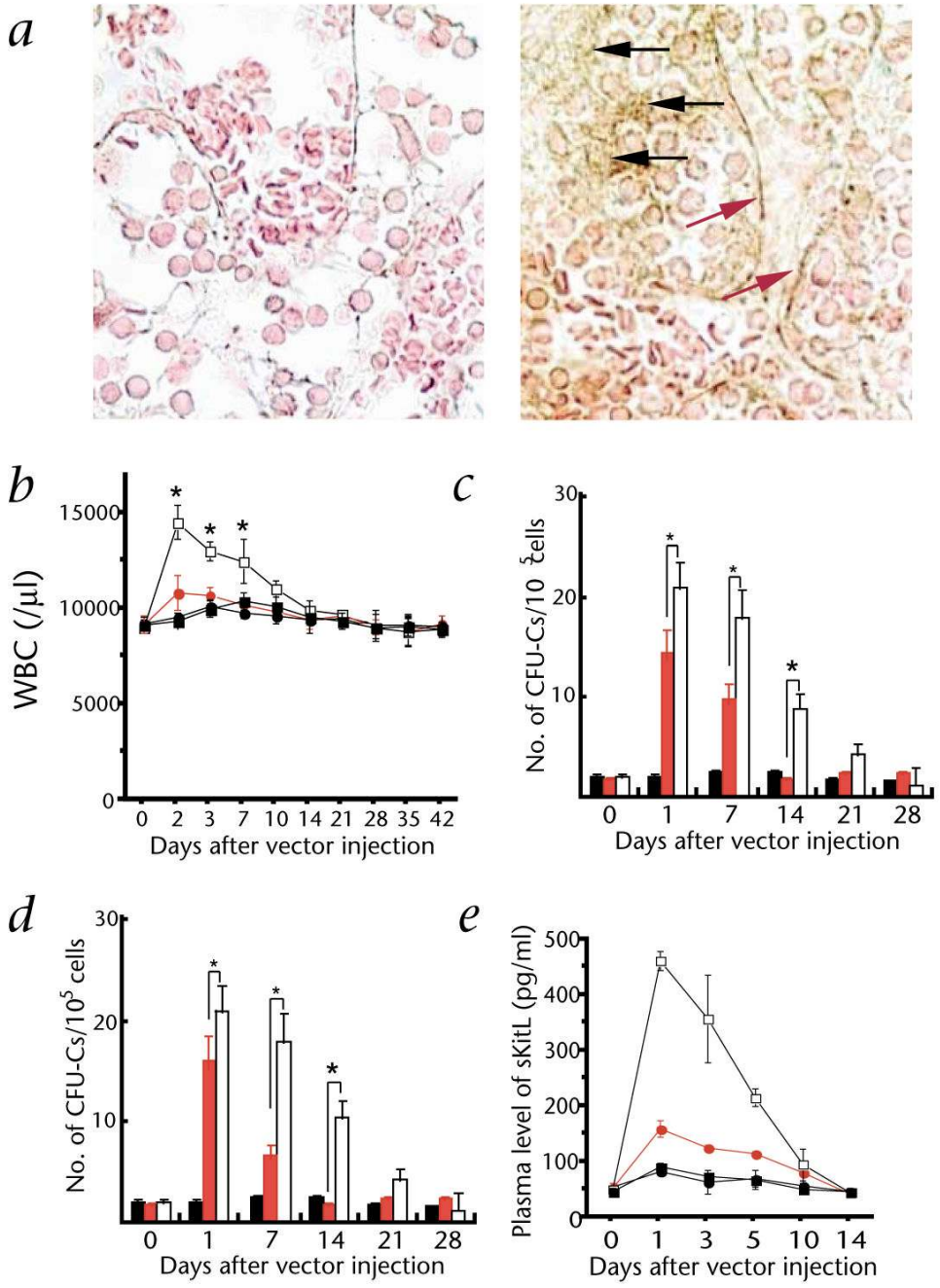

Fig. 5.

PlGF-mediated upregulation of MMP-9 and release of sKitL is essential for recruitment and mobilization of BM-repopulating cells. ***a***, Immunohistochemistry for MMP-9 (brown) of BM sections 2 d after a single-dose injection of Ad-null (left) and Ad-PlGF (right) into BALB/c mice. MMP-9 was detected in vessels (red arrows) and stromal BM cells (black arrows) 2 days after Ad-PlGF administration. Magnification × 400. ***b*–*e***, MMP-9$^{-/-}$ and MMP-9$^{+/+}$ mice[37] were injected with Ad-PlGF and/or Ad-null vector by a single i.v. dose on day 0 ($n = 6$). *b*, Total WBC counts were quantified (□, Ad-PlGF in MMP-9$^{+/+}$; ■, Ad-null in MMP-9$^{+/+}$; ●, Ad-PlGF in MMP-9$^{-/-}$; ●, Ad-null in MMP-9$^{-/-}$ mice; *, $P < 0.001$). *c*, Mobilized PBMCs were plated in a colony assay (*, $P < 0.01$). *d*, Mobilized PBMCs were injected into lethally

irradiated mice and spleen colony formation (CFU-S) was determined (*, $P < 0.01$; black bar: Ad-null in wild-type mice, red bar: Ad-PlGF in MMP-$9^{-/-}$ mice, open bar: Ad-PlGF in wild-type mice). *e*, Plasma levels of sKitL in MMP-$9^{-/-}$ and MMP-$9^{+/+}$ mice were determined by ELISA. □, Ad-PlGF in wild type; ●, Ad-PlGF in MMP-$9^{-/-}$ mice; ■, Ad-null in wild-type mice; ●, Ad-null in MMP-$9^{-/-}$ mice. Error bars represent mean ± s.e.m. for 6 mice per group (*b*) and for 3 separate experiments per variable (*c*, *d* and *e*)

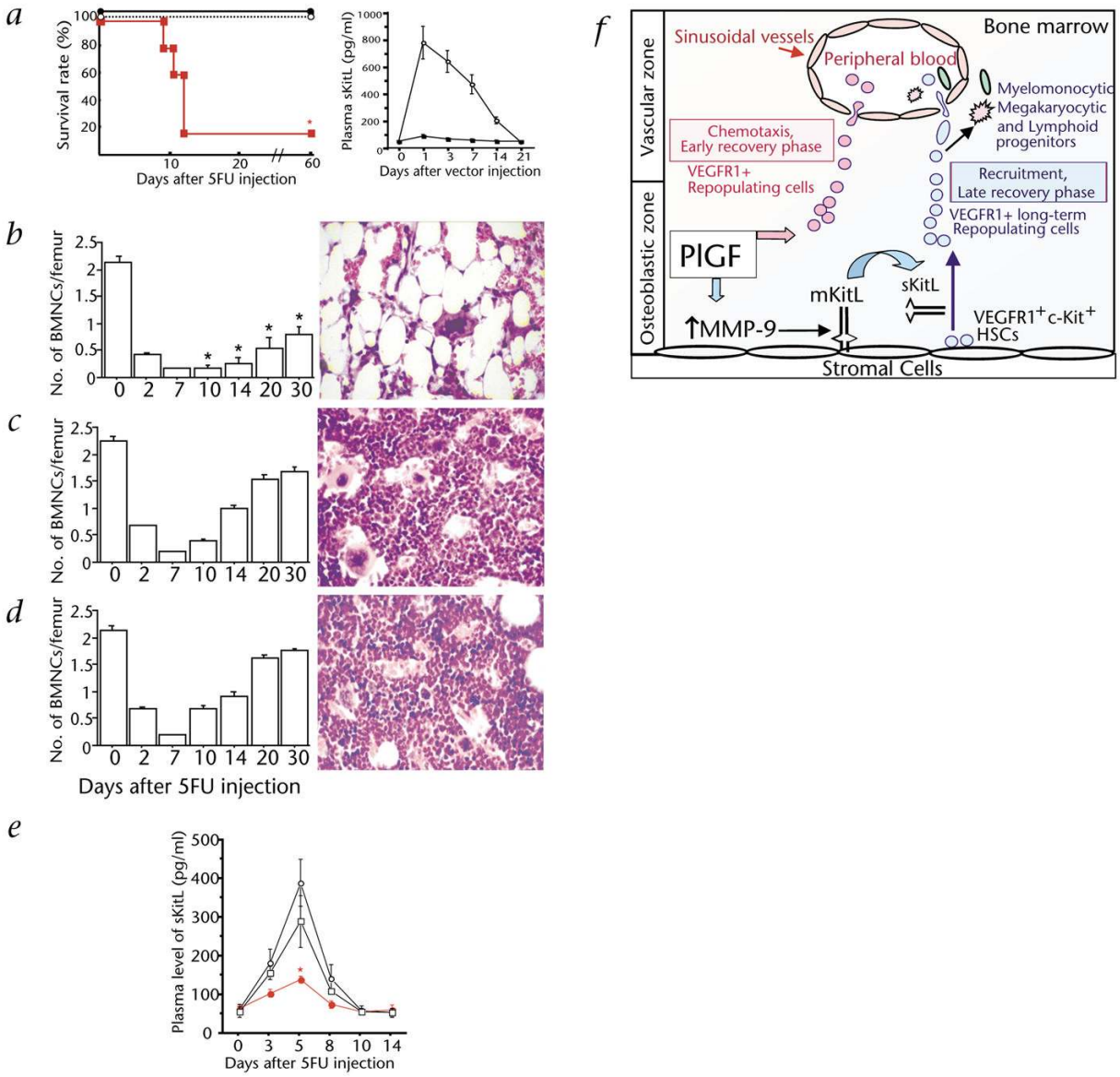

Fig. 6.

Administration of sKitL restores impaired hematopoiesis in mice treated with 5FU and neutralizing anti-VEGFR1. ***a–d***, BALB/c mice received a myeloablative dose of 5FU i.v. on day 0. Cohorts of 5FU-treated mice ($n = 6$ per group) were injected i.p. with neutralizing doses of anti-VEGFR1 or IgG (control) in 3-day intervals starting day 0. Mice were co-injected with AdsKitL or Ad-null vector on day 2. *a*, Left, Survival rates were monitored ($n = 12$; *, $P <$ 0.001). ○, 5FU+IgG+AdsKitL; ●, 5FU+anti-VEGFR1+AdsKitL; ■, 5FU+anti-VEGFR1. Right, Plasma levels of sKitL were determined by ELISA. ○, AdsKitL; ■, Ad-null. *b–d*, BMMCs were counted and H&E staining of femurs of anti-VEGFR1 (*b*), anti-VEGFR1 +AdsKitL (*c*) and AdsKitL-treated (*d*) mice was performed for morphological analysis, magnification, ×400. *, $P < 0.01$ comparing the absolute number of BMMCs in the anti-VEGFR1 vs. the control groups. ***e***, Plasma sKitL levels were measured by ELISA in 5FU-treated mice co-injected with neutralizing doses of mAb to VEGFR1 or IgG ($n = 5$; *, $P < 0.01$ comparing sKitL plasma levels in mice treated with anti-VEGFR1 to controls). ○, 5FU+IgG;

●, 5FU+anti-VEGFR1; □, 5FU+anti-VEGFR2. ***f***, PlGF mediates the early phase of BM recovery through rapid mobilization/chemotaxis of preexisting VEGFR1$^+$ BM-repopulating cells. During the late phase of BM recovery PlGF promotes hematopoiesis primarily through MMP-9 mediated release of sKitL, resulting in enhanced cell motility, cycling and differentiation of VEGFR1$^+$ long-term repopulating cells. Error bars represent mean ± s.e.m. for 2–-5 separate experiments (*a–e*).